PROBLEMY MECHATRONIKI
UZBROJENIE, LOTNICTWO, INŻYNIERIA BEZPIECZEŃSTWA

ISSN 2081-5891

10, 1 (35), 2019, 99-120

PROBLEMS OF MECHATRONICS
ARMAMENT, AVIATION, SAFETY ENGINEERING

Changes in Mechanical Properties of Ultrahigh Strength Nanostructured Steel Resulting from Repeated High Strain Rate Deformation

Jarosław MARCISZ[1*], Bogdan GARBARZ[1], Jacek JANISZEWSKI[2]

[1]Institute for Ferrous Metallurgy, 12-14 K. Miarki Str., 44-100 Gliwice, Poland
[2]Military University of Technology, Faculty of Mechatronics and Aerospace, 2 gen. Witolda Urbanowicza Str., 00-908 Warsaw, Poland
Corresponding author's e-mail address and ORCID:
jmarcisz@imz.pl; https://orcid.org/0000-0002-0001-2197

Received by the editorial staff on 6 July 2018
The reviewed and verified version was received on 22 February 2019

DOI 10.5604/01.3001.0013.0800

Abstract. The paper contains results of investigation of nanostructured bainitic steel subjected to repeated high-strain-rate deformations using split Hopkinson pressure bar method and uniaxial compression of cylindrical specimens in Gleeble simulator. Steel of chemical composition Fe-0.58%C-1.80%Si-1.95%Mn-1.3Cr-0.7Mo (weight %), after isothermal heat treatment at 210°C, is characterized by following mechanical properties determined at static tensile test: yield strength $YS_{0.2}$ = 1.3 GPa; ultimate tensile strength UTS = 2.05 GPa; total elongation E = 12%, hardness 610 HV and Charpy-V impact toughness 24 J at +20°C and 14 J at -40°C. Stress-strain curves obtained for pre-stressed material before the next dynamic compression and after repeated compressions were analysed.

.

Microstructure of the deformed specimens in areas of the dynamic impact was investigated. The effects of the dynamic repeated impact on changes in characteristics of the investigated material, in that on strain hardening mechanism, were established. Critical strains of 5.3% at strain rate 910 s^{-1} and about 10% at strain rate 50 s^{-1} for the nanostructured bainite were determined. Exceeding the critical strain under uniaxial repeated high-strain-rate compression, resulted in decreasing of ability of the steel for further plastic deformation and strain hardening.
Keywords: materials engineering, nanostructured steel, dynamic deformation, adiabatic shear bands

1. INTRODUCTION

Nanostructured bainitic steel with the tensile strength of at least 2.0 GPa, yield strength of at least 1.3 GPa and total elongation of at least 12% is a material with a potential for use in ballistic protection. Assessment of armour steel grade suitability includes a number of standardised tests, in particular, qualification firing tests. An important criterion is the result of the multi-hit firing test, where the material is subjected to repeated high-energy impact loadings, with a specific distance between neighbouring impact points. The changes occurring in the microstructure and properties of the material as a result of repeated firing, and their range, are key characteristics of armour steel grade and decide on its suitability as shield against penetration by armour piercing ammunition. For this reason, the authors decided to address the issue of characteristic changes in materials subjected to multiple dynamic loading.

Studies of dynamic properties are conducted to determine the parameters of production processes (e.g. plastic working technologies) or to reproduce the conditions under which a material (e.g. an anti-impact shield) is used, where loads characterised by high strain rate occur. The nature of dynamic loads is defined based on the strain rate value [1, 2]. It is assumed that dynamic tests are performed at strain rate within the $1 \div 10^5$ s^{-1}, and above 1×10^5 s^{-1} they are considered impact loads [1]. Experimental testing of dynamic properties is conducted by compression, torsion, shearing and tension of samples, and the test result analysis utilises the theory of elastic wave propagation in the material. In the case of impact loadings, the phenomenon of shockwave propagation occurs, e.g. in explosion and firing tests. Quasi-static tests (e.g. static tensile or compressive tests) are conducted at strain rate from 10^{-4} to 1 s^{-1}. Strain rates lower than 10^{-4} s^{-1} occur in creep and stress relaxation processes. Significant differences in material reaction to deformation between quasi-static and dynamic tests concern, among others, the effects of strain rate on plastic flow stress values, deformation heat generation processes and methods of its conduction, or hardening mechanisms and forming and type of deformation heterogeneity [3].

A common material testing technique for high strain rate is the split Hopkinson pressure bar (SHPB), also called the Kolsky bar [4-6]. Impact on the sample surface does not occur in the SHPB dynamic uniaxial compression test. The Taylor test is also used, which involves colliding a cylindrical sample with the flat surface of a target shield [4]. The Taylor test involves the phenomenon of impact on the sample surface. Within the lower strain rate range (up to approx. 300 s^{-1}), compression, tensile and shear tests can be performed using hydraulic testing machines, e.g. the metallurgical process simulator Gleeble. In this case, the strain rate depends largely on sample geometry. In all the above mentioned examination methods, stresses and strains are non-uniformly distributed in the loaded sample. This phenomenon is particularly important when using high strain rates and high energies per unit area. Characteristic properties of interactions under high strain rates, including impacts, are: stress and strain localisation, caused by the phenomenon of tool friction with the sample surface, limited carrying away of heat and distribution of stresses resulting from the geometry and dimensions of the sample-tool configuration.

Problems concerning tests focused on specific applications of nanostructured bainitic steels have in recent years been the subject of many projects and analyses conducted by research institutions around the world. Nanobainitic steel investigations have been conducted in European research centres for several years. It is impossible to analyse all available papers and other materials (e.g. research project reports) in detail due to their great numbers, and the detailed nature of both research and technology issues addressed. The first studies and theoretical analyses which indicated the possibility of producing nanostructured bainite were conducted by the Christian, Edmonds and Bhadeshia team in 1980–1990 [7-10], while later papers by Bhadeshia et al. concerned technological issues and potential applications of nanobainitic steel, e.g. [11-12].

At the Institute for Ferrous Metallurgy (Gliwice, Poland), studies of this steel grade group began in 2008 with a research and development project financed from structural funds [13, 14]. As a result of the project, the chemical composition and method of producing nanobainitic steel named NANOS-BA® were patented [15]. The next stage of the studies was a project covering the implementation preparation stage for commercial application of NANOS-BA® steel plates in armour elements [16]. In 2017–2020, another implementation project is being carried out, involving the use of nanostructured bainitic steel plates in the armour system for observation and defence containers [17].

2. INVESTIGATED MATERIALS

The examination were performed on bainitic nanostructured steel Fe-0.58%C-1.80%Si-1.95%Mn-1.3Cr-0.7Mo (wt. %) following isothermal annealing at 210°C.

As a result of the heat treatment applied, the following mechanical properties were achieved: yield strength $YS_{0.2}$ = 1.3 GPa; ultimate tensile strength UTS = 2.05 GPa; total elongation E = 12%, hardness 610 HV and impact strength KV at +20°C = 24 J and KV at -40°C = 14 J. Fig. 1 shows macrostructure and hardness distribution on the cross-section of the sample subjected to dynamic deformation. The steel microstructure consisted of carbide-free nanolaths of bainite and 20% retained austenite in the form of thin layers between bainite laths, and as sub-micron grains (Fig. 2). The studies of dynamic properties of this steel performed to date involved standard compression and shear tests using the SHPB method and using the Gleeble simulator, and firing tests.

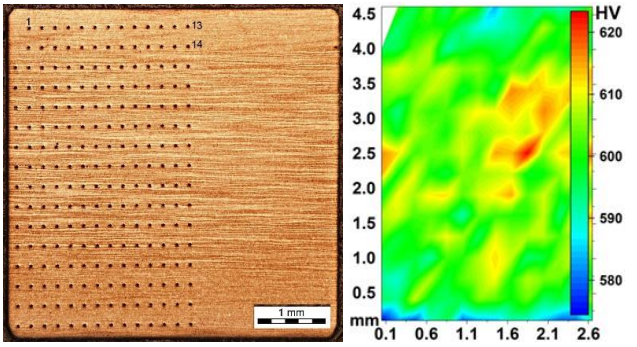

(a) (b)

Fig. 1. Macrostructure (a) and hardness distribution (b) in a cross-section of the sample subjected to deformation

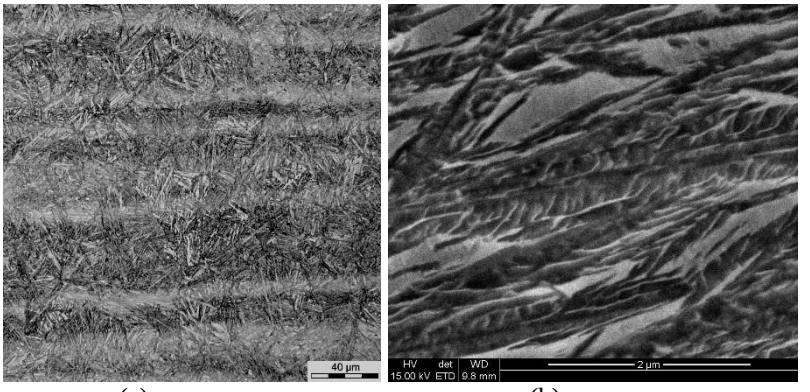

(a) (b)

Fig. 2. Microstructure of the sample subjected to dynamic deformation (a) light microscope, (b) scanning electron microscope

The NANOS-BA® steel is characterised by a high dynamic yield strength of approx. 2.7 GPa at strain rate 4300 s^{-1} and shear stress of 1.5 GPa at punch velocity 10 m/s.

In firing tests of plates with 8.0 mm nominal thickness, made of nanostructured bainitic steel, the requirements specified for level 2 in STANAG 4569 were met [18-22].

3. EXAMINATION METHODS

Tests under repeated high-strain-rate loading conditions were conducted using a split Hopkinson pressure bar and Gleeble simulator. In both cases, uniaxial compression of cylindrical samples was performed. The first of the above examination methods enables achieving strain rate within the range of $10^2 \div 10^4$ s^{-1}, while the simulator enables strain rate up to 10^2 s^{-1}.

3.1. Deformation using the split Hopkinson pressure bar

Repeated deformation was carried out using uniaxial compression of cylindrical samples with diameter of 4.0 and 5.0 mm, and with a height of 5.0 mm. The time between subsequent deformations was selected, so it ensured that ambient temperature was reached in the entire sample volume before the next compression. Variable experiment parameters were strain value and strain rate (Table 1). These parameters are correlated with each other in such a manner that higher strain rate was used to achieve greater strain. Samples with a diameter of 4.0 mm enable achieving greater strain values and strain rates than when compared to 5.0 mm diameter samples. Tests were conducted until sample shear (crack) was achieved during the second or third deformation stage. The maximum total strain value was 0.16.

Table 1. Repeated high strain rate deformation test parameters with the use of the split Hopkinson pressure bar

Sample diameter/ length (*do*/*lo*)	**Strain ε_1**	**Strain rate $\dot{\varepsilon}_1$**	**Strain ε_2 (ε_3)**	**Strain rate $\dot{\varepsilon}_2$ ($\dot{\varepsilon}_3$)**	**Total strain**	
mm	**%**	**s^{-1}**	**%**	**s^{-1}**	**(*lo*-*l*)/*lo*, %**	**ln (*l*/*lo*)**
5 / 5	3.5	550	6.0	870	9.2	0.097
5 / 5	8.5	1070	1.2	320	9.0	0.094
5 / 5	8.8	1300	2.7	490	12.0	0.128
4 / 5	5.3	910	7.6	1070	12.2	0.130
4 / 5	11.5	1900	4.3	1160	14.8	0.160
4 / 5	12.3	1640	1.4 (4.2)	550 (1260)	*	*

*) sample failure (adiabatic shear)

3.2. Deformation using the Gleeble simulator

The Gleeble simulator was used to perform uniaxial double compression at a constant strain rate of 50 s^{-1}. The experiments were carried out using cylindrical samples with a diameter of 5.0 mm and a height of 5.0 mm, for which total strain of 0.45 and 0.50 was achieved. The time between the first and second stage of deformation was 30 s, which ensured that the sample and the die would revert to the ambient temperature before the next compression. The parameters of compression experiment are provided in Table 2.

Table 2. Parameters of repeated dynamic deformation test with the use of the Gleeble simulator at strain rate 50 s^{-1}

Sample diameter/length (*do*/*lo*)	**Strain ln (*l*/*lo*)**		**Total strain**	
	ε_1	ε_2		
mm	-	-	$\varepsilon_1+\varepsilon_2$	**(*lo*-*l*)/*lo*, %**
5 / 5	0.12	0.33	0.45	36
5 / 5	0.25	0.25	0.50	40
5 / 5	0.35	0.15	0.50	40

During the compression, the temperature was measured using a thermocouple welded to the side surface of the sample. Fig. 3 shows the temperature measurement results. Sample surface temperature after the first compression increased to 75, 150 and 200°C for strain values 0.12; 0.25 and 0.35 respectively. Similarly the second compression caused an increase in temperature to approx. 100, 150 and 200°C for strain 0.15, 0.25 and 0.33 respectively.

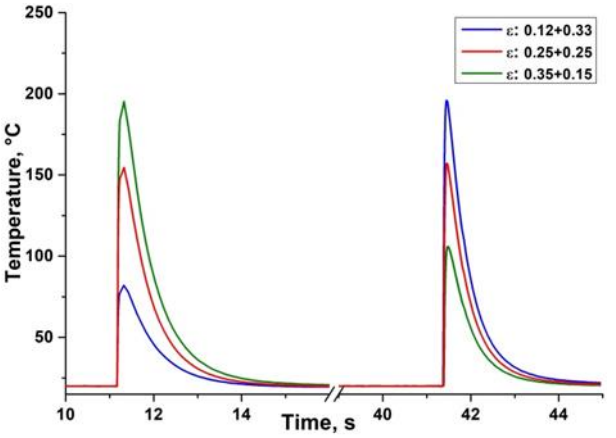

Fig. 3. Temperature change on the side surface of the sample resulting from double dynamic compressions in the Gleeble simulator

4. EXAMINATION RESULTS

4.1. Results of repeated high-strain-rate deformation using the Hopkinson technique

As a result of dynamic compression using the Hopkinson technique, stress-strain curves within the strain rate range of 300-1900 s^{-1} were determined. Hardening mechanism of nanostructured bainitic steel is the deformation-induced transformation of retained austenite into martensite. Occurrence of this transformation depend on strain value and strain rate, and on strain uniformity within the sample. Figs. 4-6 show compression curves for samples with a 5.0 mm diameter, for strain rate up to 1300 s^{-1}. The material initially deformed by 3.5% at a strain rate of 550 s^{-1} and then 6.0% at a strain rate of 870 s^{-1} did not crack. The profile of the compression curves indicated a slight hardening effect in the first deformation cycle, while in the second cycle, the stress was greater and did not change with strain increasing (Fig. 4).

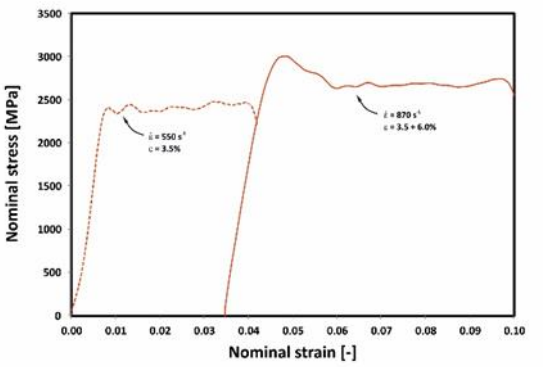

Fig. 4. Dynamic stress-strain curves obtained as a result of double compression under SHPB test conditions. Sample with a 5.0 mm diameter

The increasing stress level during the second compression stage resulted from work hardening during the first compression stage, caused by the transformation of some of the retained austenite into martensite, increased dislocation density, and – after exceeding critical strain rate and strain value – formation of adiabatic shear bands. At the same time, the retained austenite, remaining before the second deformation, stabilised itself to such a degree that during the next deformation stage it did not cause increased stress due to transformation into martensite with progressing compression. Figs. 5 and 6 show compression curves, for which during the first strain of 8.5 and 8.8% were achieved at strain rate of 1070 and 1300 s^{-1} respectively. As a result of the dynamic deformation, the material exhibited distinct hardening, indicating retained austenite transformation into martensite.

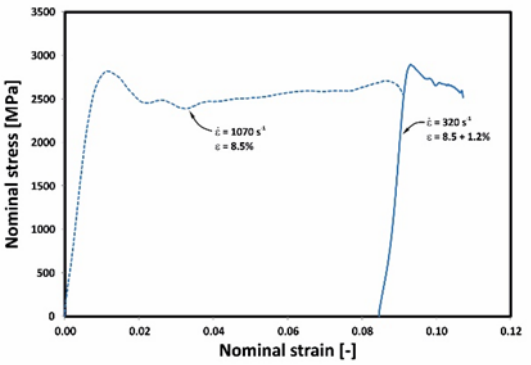

Fig. 5. Dynamic stress-strain curves obtained as a result of double compression under SHPB test conditions. Sample with a 5.0 mm diameter

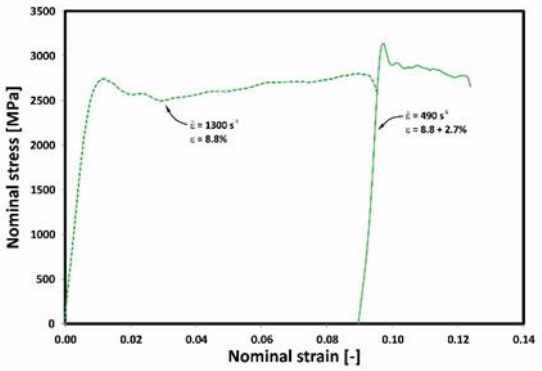

Fig. 6. Dynamic stress-strain curves obtained as a result of double compression under SHPB test conditions. Sample with a 5.0 mm diameter

Following deformation, with values of 1.2 and 2.7% at a strain rate of 320 and 490 s^{-1} respectively, initially caused increased stress levels, and subsequently a clear drop as compression progressed. In this case, the effect of stress value decreasing reduction occurred, caused by a local increase in material temperature, among others. Moreover, after the first deformation stage, a more stable retained austenite remained, which in the second compression stage transformed into martensite to a minor degree.

For samples with 4.0 mm diameter, higher strain rate were reached. Double compression curves with the first strain of 5.3% at a strain rate of 910 s^{-1} and second strain of 7.6% at a strain rate of 1070 s^{-1} showed a significant increase in stress and a lack of hardening in the second compression stage, without a stress drop effect (Fig. 7). For the first deformation of 11.5% at a strain rate of 1900 s^{-1}, the repeated deformation of 4.3% at a strain rate of 1160 s^{-1} caused a noticeable stress drop effect (Fig. 8).

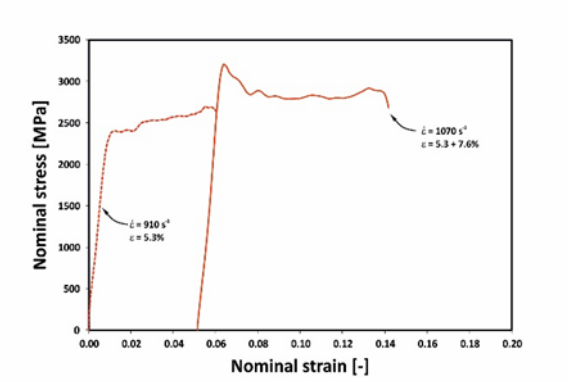

Fig. 7. Dynamic stress-strain curves obtained as a result of double compression under SHPB test conditions. Sample with a 4.0 mm diameter

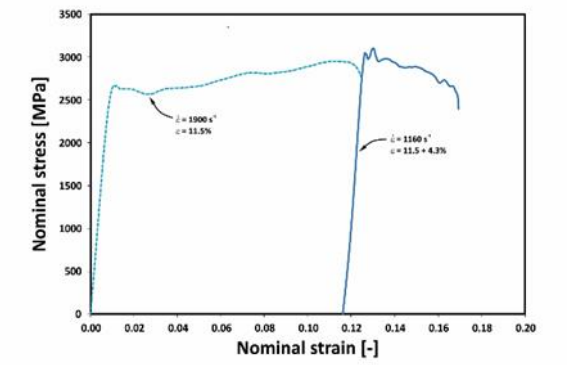

Fig. 8. Dynamic stress-strain curves obtained as a result of double compression under SHPB test conditions. Sample with a 4.0 mm diameter

Pre-hardened material, where austenite partially transformed into martensite, losses the ability for further work hardening due to the limited ability of the remaining retained austenite to transform into martensite, and due to the reduced density of mobile dislocations, caused by annihilation and pinning processes during the first deformation stage. The total effect causing the stress decreasing, resulting from a local temperature increase, formation of shear bands or microcracks, significantly exceeds the work hardening effect. Fig. 9 shows triple compression curves of a material that cracked during third stage of dynamic compression. During the first compression stage, by causing a strain of 12.3% at a strain rate of 1640 s^{-1}, a work hardening effect was occurred. During the next stage, after strain of 1.4% at a strain rate of 550 s^{-1}, the material was still capable of hardening. The third compression stage was performed by strain of 4.2% at a strain rate of 1260 s^{-1}. During this process, stress dropped significantly and the sample was sheared.

The cause of this phenomenon was the strain localisation, causing formation of adiabatic shear bands, which preceded sample cracking.

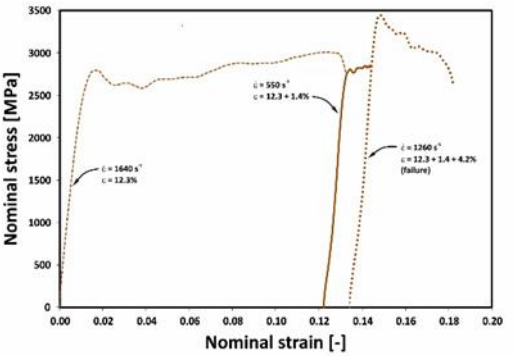

Fig. 9. Dynamic stress-strain curves obtained as a result of triple compression under SHPB test conditions. Sample with a 4.0 mm diameter

4.2. Results of micro- and macrostructure examination and hardness measurements following deformations under SHPB test conditions

Following repeated high-strain-rate deformation, the samples were subjected to macro- and microstructure examination and hardness distribution in a cross-section parallel to the shearing direction was determined. Areas where hardness exceeded 700 HV were found. In samples that did not crack, matrix hardness (outside the areas with the highest hardness) increased to the range of 660-680 HV (Figs. 10-12). In the sample that cracked as a result of triple dynamic compression, adiabatic shear bands were found on the crack surface, and sample matrix hardness increased to approx. 690 HV (Fig. 13). Samples with a 5.0 mm diameter, compressed at a lower strain rate compared to 4.0 mm diameter samples, were characterised by greater deformation uniformity, determined on the basis of hardness distribution. The zone of higher hardness was located in the middle of the sample's height (Fig. 11). For 4.0 mm diameter samples, shear zones – typical for compression tests – were found to be located near the edge of the cylinder's base, angled at approx. 45° against the compression direction (Fig. 12). In the strain localisation areas, adiabatic shear bands and cracks were found. Based on microstructure examination using a light microscope, no visible changes in morphology were found, other than a reduction in distances between segregation bands along the compression direction.

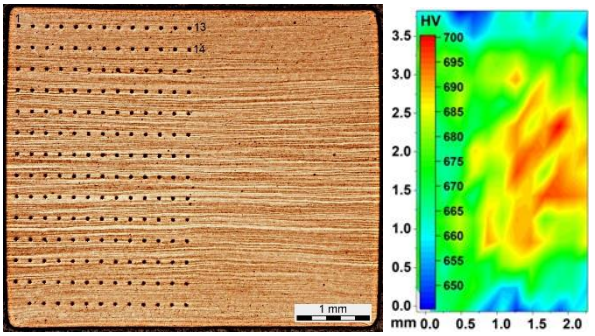

Fig. 10. Macrostructure and hardness distribution following double dynamic deformation. 5.0 mm diameter sample; strain (%)/strain rate (s^{-1}): 3.5/550+6.0/870

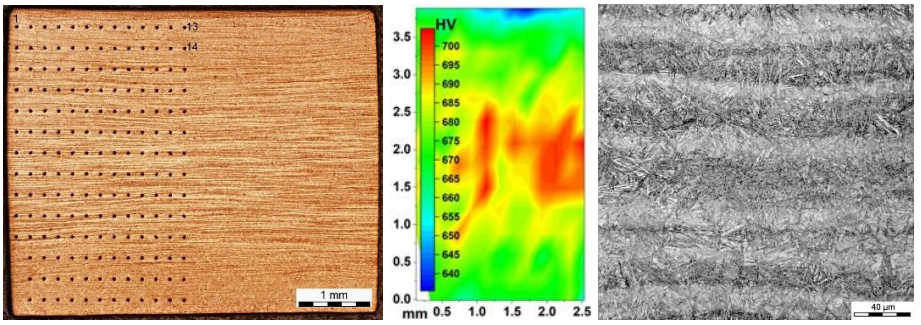

Fig. 11. Macrostructure, microstructure and hardness distribution following double dynamic deformation. 5.0 mm diameter sample; strain (%)/strain rate (s^{-1}): 8.8/1300+2.7/490

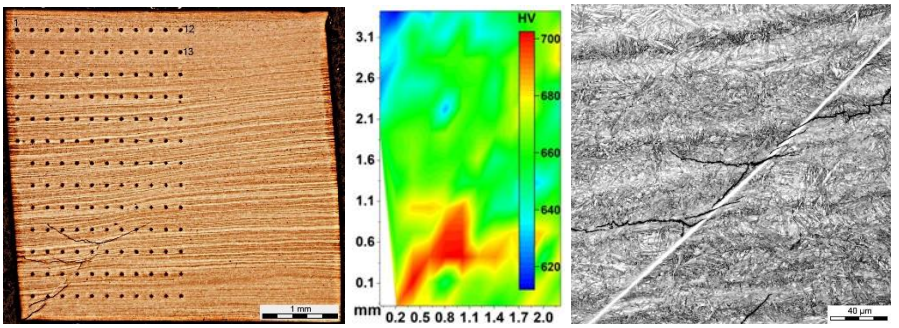

Fig. 12. Macrostructure, microstructure and hardness distribution following double dynamic deformation. 4.0 mm diameter sample; strain (%)/strain rate (s^{-1}): 11.5/1900+4.3/1160

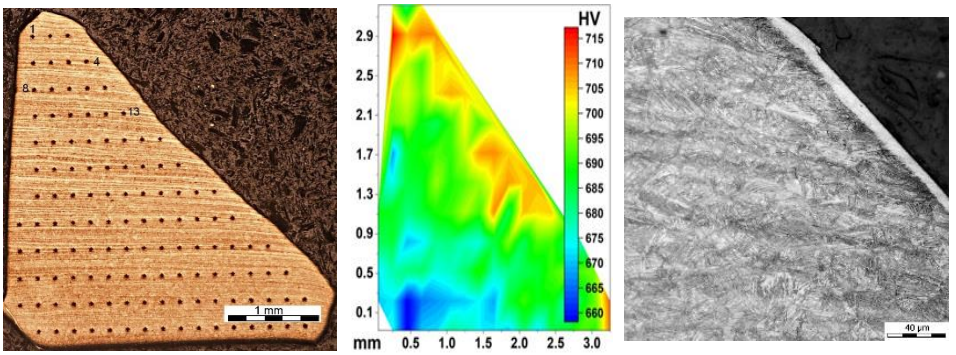

Fig. 13. Macrostructure, microstructure and hardness distribution following triple dynamic deformation. 4.0 mm diameter sample; strain (%)/strain rate (s^{-1}): 12.3/1640+1.4/550+4.2/1260

4.3. Results of repeated dynamic deformation using the Gleeble simulator

During the first compression tests, critical strain values for sample cracking were determined. Sample strain at a strain rate of 50 s^{-1}, single with a value of 0.60 and double with a total value of 0.55 (0.35+0.20), resulted in sample cracking. Fig. 14 shows double compression curves, which resulted in sample cracking (continuous line – strain 0.35+0.20), and when the sample did not crack (dotted line – strain 0.35+0.15).

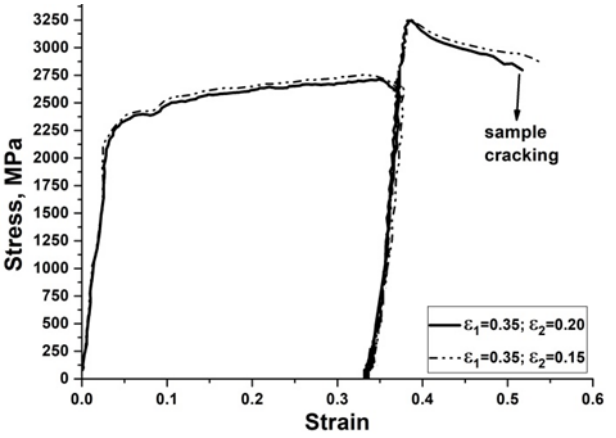

Fig. 14. Dynamic stress-strain curves obtained as a result of double compression using the Gleeble simulator. Sample with a 5.0 mm diameter

Fig. 15 shows double dynamic compression curves with the first strain of 0.12 and the second strain of 0.33. The shape of the compression curves in relation to work hardening during the second deformation stage did not change significantly, compared to material compressed only once, other than a minor increase in stress level.

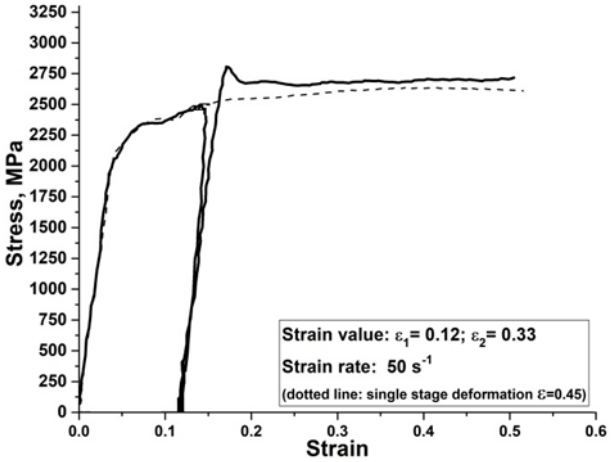

Fig. 15. Dynamic stress-strain curves obtained as a result of double compression using the Gleeble simulator. Sample with a 5.0 mm diameter

A significantly different behaviour of the steel was observed in double compression experiment for which the strain during the first stage was 0.25 and 0.35, and in the second stage 0.25 and 0.15 respectively (Figs. 16 and 17). During the first compression, the material was hardened as a result of partial transformation of austenite into martensite, and due to increased dislocation density. Retained austenite is richer in carbon, compared to the bainitic matrix and mean carbon content in the steel. Before the second deformation, the steel was characterised by a microstructure composed of carbide-free lower lathy bainite (nanobainite), retained austenite and high-carbon martensite formed from a part of the retained austenite (so called "fresh martensite"). The material in such a structural state has no work hardening ability, and stress reduces with increasing strain during compression, as a result of local temperature increase and structural changes.

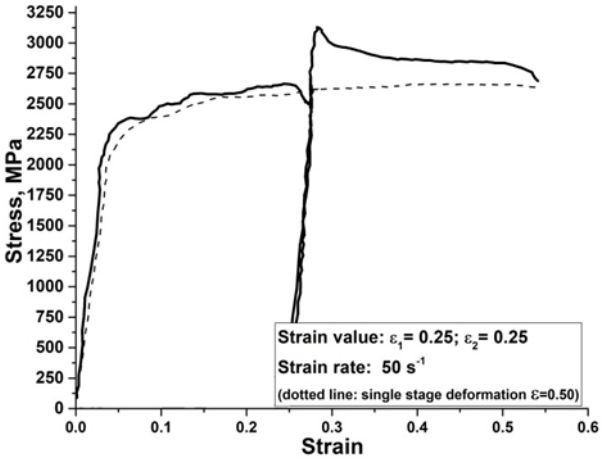

Fig. 16. Dynamic stress-strain curves obtained as a result of double compression using the Gleeble simulator. Sample with a 5.0 mm diameter

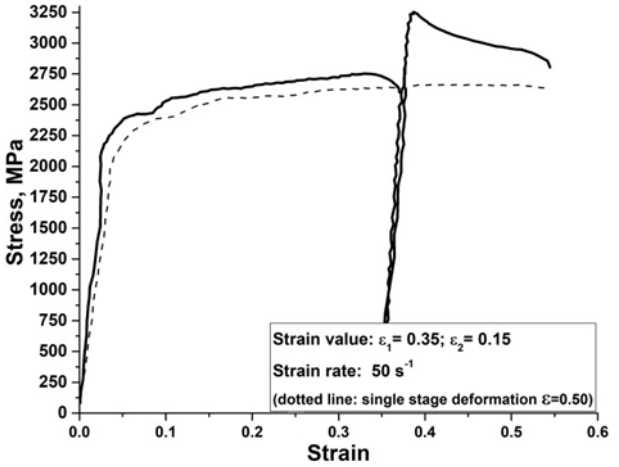

Fig. 17. Dynamic stress-strain curves obtained as a result of double compression using the Gleeble simulator. Sample with a 5.0 mm diameter

4.4. Results of micro- and macrostructure examination and hardness measurements following deformations using the Gleeble simulator

Samples deformed in the Gleeble simulator were subjected to macro- and microstructure examination and hardness distribution in a cross-section parallel to the direction of compression was determined. Fig. 18 shows macrostructure and microstructure, and hardness distribution of a sample compressed once to a strain value of 0.60.

Adiabatic shear bands were found in the specimen, which caused specimen failure. The results of macro- and microstructure, as well as sample hardness measurements after double uniaxial compression are shown in Figs. 19-21. Areas where hardness reached 800 HV were identified. In this material, no adiabatic shear bands were found.

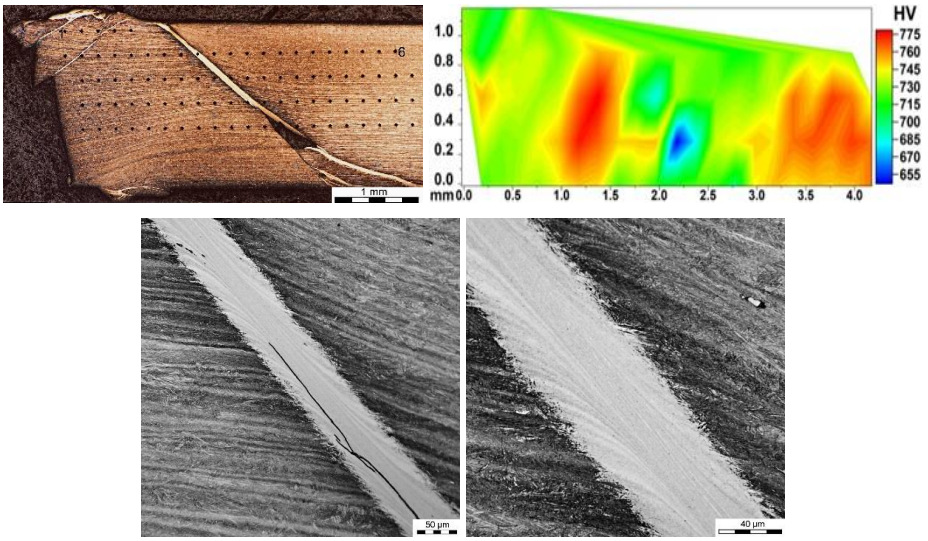

Fig. 18. Macrostructure, microstructure and hardness distribution after single dynamic deformation at strain rate of 50 s^{-1}. 5.0 mm diameter sample; strain 1.0

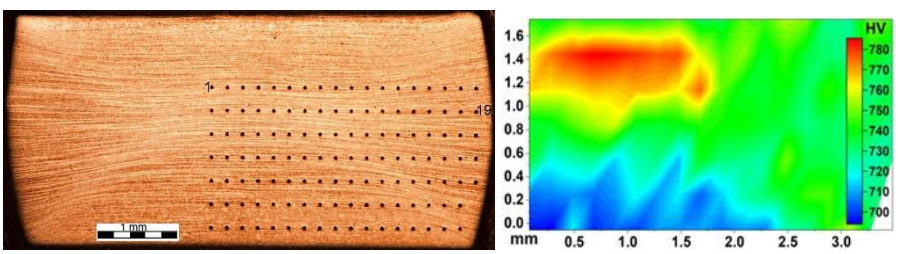

Fig. 19. Macrostructure and hardness distribution after double dynamic deformation at strain rate of 50 s^{-1}. 5.0 mm diameter sample; strain: 0.12+0.33

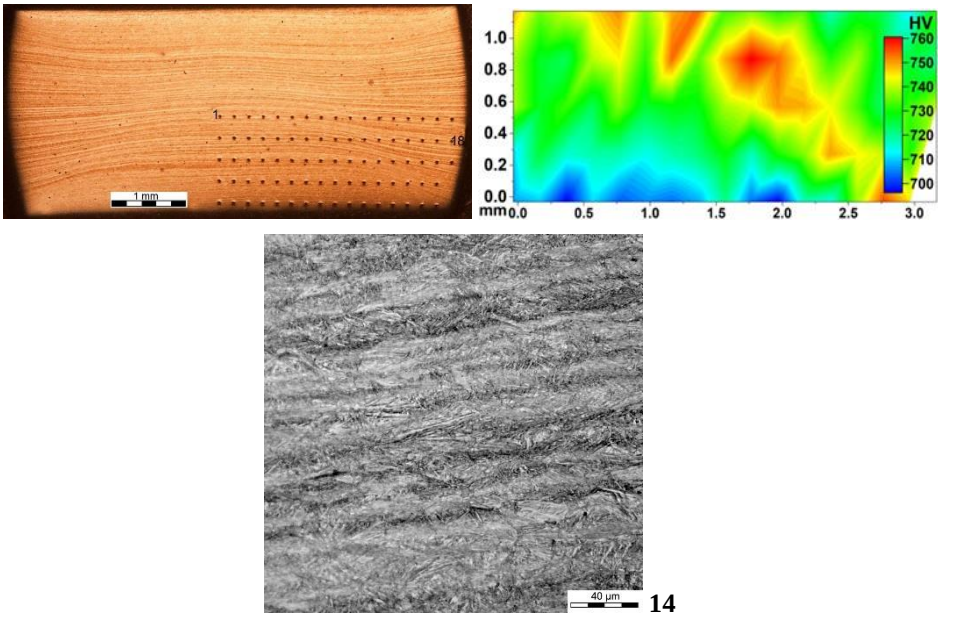

Fig. 20. Macrostructure, microstructure and hardness distribution after double dynamic deformation at strain rate of 50 s^{-1}. 5.0 mm diameter sample; strain: 0.25+0.25

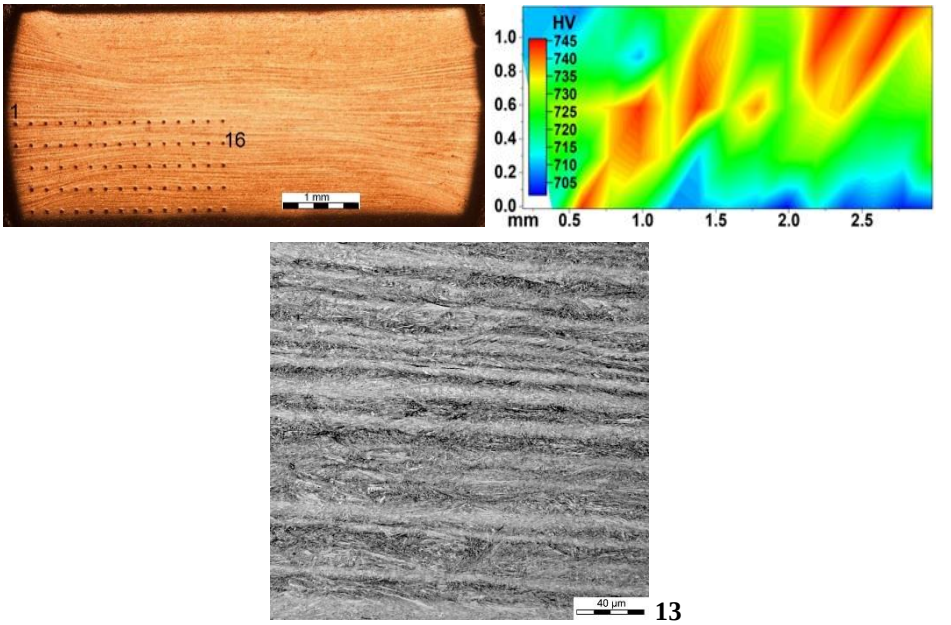

Fig. 21. Macrostructure, microstructure and hardness distribution after double dynamic deformation at strain rate of 50 s^{-1}. 5.0 mm diameter sample; strain: 0.35+0.15

5. SUMMARY OF EXAMINATION RESULTS AND DISCUSSION

Repeated high-strain-rate uniaxial compression experiments were conducted on nanostructured bainitic steel in a wide range of strain rate: 300-1900 s^{-1} using the split Hopkinson pressure bar and 50 s^{-1} in the Gleeble simulator. For the above strain rate ranges, critical strain values were determined, which – if exceeded – would result in the material significantly changing its properties, in particular, its work hardening capability and ductility. Microstructural changes occurring in the material as a result of dynamic deformation were analysed, taking into account the effects of strain localisation during the compression.

Nanostructured bainitic steel, when compressed to a strain value of 5.3% at a strain rate of 910 s^{-1}, exhibits a constant stress level with increasing strain during in its next compression. Applying the first deformation of strain value of 8.5% at strain rate of 1070 s^{-1} causes significant changes in the material's mechanical properties. Nanostructured steel is then characterised by a microstructure composed of carbide-free bainite supersaturated with carbon, retained austenite with a high carbon content due to diffusion of this element during a long-lasting isothermal transformation, and high-carbon martensite formed from retained austenite as a result of a deformation-induced phase transformation (TRIP effect). Non-uniform distribution of carbon in the bainite and austenite results from the difference in this element's solubility in the above phases.

This type of material exhibits a marked drop in stress during deformation. At strain rate of 50 s^{-1}, the first compression with a strain value of 0.12 (approx. 10%) causes such changes in the material, that during the repeated deformation to strain value of 0.33 (approx. 25%), the material flows under constant flow stress. On the other hand, the first deformation with a strain value of 0.25 (approx. 20%) results in a significant change in mechanical properties. During the next stage of high-strain-rate compression, the steel displays a drop in stress with increasing strain level. Steel microstructure changes as a result of dynamic deformation involve an increase in dislocation density and a deformation-induced transformation of retained austenite into martensite. The volume fraction of austenite that does not transform during initial compression, and the propensity of the remaining austenite for phase transformation are key factors that decide the material's behaviour under repeated high-strain-rate deformation. The localisation of the stress causing shear bands formation, which may decide the material's properties, is not without importance as well. A detailed analysis of microstructure changes was not a subject of the study and will be continued.

As a result of double dynamic deformation under the split Hopkinson pressure bar test conditions, a local increase in hardness from the initial value of 610 HV to a maximum of approx. 700 HV was achieved.

In uniaxial compression tests, this method minimises the effects of friction between forward surfaces of the sample in contact with the compression bars on deformation heterogeneity. In the case of compression using the Gleeble simulator, hardness increased locally to 800 HV. In this method, the friction phenomenon is the cause of deformation heterogeneity within the volume of the cylindrical sample. Hardness of the martensite in the examined steel with a carbon content of approx. 0.60% based on dilatometric study is approx. 770 HV. Hardness of the non-deformed bainitic and austenitic matrix is approx. 610 HV. Given the above, the increase in hardness results from the presence of high-carbon martensite formed in the deformation-induced transformation from retained austenite, and from the increase in dislocation density in bainite laths and in the remaining retained austenite.

In the process of dynamic deformation of nanostructured bainitic steel, opposite – from the perspective of steel hardening – phenomena occur: a strain-induced transformation of high-carbon retained austenite into martensite, and an increase in dislocation density, resulting in increased stresses and localisation of deformation, e.g. in form of adiabatic shear bands, which cause a temperature increase and stress drop (so-called thermal softening effect). The impact of the above phenomena decided the total hardening or material softening effect, or in extreme cases, the occurrence of a constant stress level with increasing strain. These phenomena also cause changes in material ductility and its ability to energy absorption or change the type of microstructure, among others. Furthermore, the tendency to transformation of retained austenite or increase dislocation density is highly dependent on strain rate and deformation method, including the material's propensity for stress and strain localisation. In nanostructured bainitic steel, retained austenite occurs as thin layers between bainite laths, and as small grains. Mechanical and thermodynamic stability of austenite significantly depends on its carbon content and on its morphology and arrangement in relation to other elements of the microstructure. The assessment of the influence of retained austenite on the mechanical behaviour of nanostructured bainitic steel during dynamic deformation, including repeated high-strain-rate deformation, requires further advanced material studies to determine the volume fraction of individual morphological types of this phase, and to determine the carbon content.

6. CONCLUSIONS

The main conclusions from the examination performed are as follows:

- When designing materials intended for ballistic protection, the effects of subsequent deformations caused by overlapping multiple dynamic interactions must be characterised quantitatively and taken into account.

- For the types and values of repeated uniaxial dynamic compression applied in the study, the occurrence of critical strain was found, which when applied, resulted in the material losing its ductility and work hardening ability (energy absorption) during the next high-strain-rate deformation. The critical strain value for nanostructured steel depends on strain rate and equals 5.3% at 910 s^{-1} and approx. 10% at 50 s^{-1}.
- Based on current knowledge, it can be concluded that one method of increasing the ability to absorb the energy of dynamic interactions in subsequent deformations is to produce a material with an increased work hardening potential while maintaining other required parameters, e.g. cracking resistance. A method of increasing the work hardening potential of nanostructured bainitic steel while maintaining ductility is to produce, through an isothermal transformation, a thermodynamically and mechanically stable retained austenite in the form of laths separating bainite laths.

The paper contains the results of examination conducted under a project finances from structural funds POIR 04.01.04.-00-0047/16, entitled: Development of production technology of light observation-protective container (LOOK) made of nanostructured ultrahigh strength steels

REFERENCES

[1] Kurzydłowski J. Krzysztof. 1993. *Mechanika materiałów*. Warszawa: Wydawnictwo Politechniki Warszawskiej.

[2] Nowacki K. Wojciech. 1996. „Badanie własności dynamicznych materiałów konstrukcyjnych przy dużych prędkościach deformacji". *Przegląd Mechaniczny* 23-24 : 14.

[3] Meyers Marc Andre. 1994. *Dynamic Behavior of Materials*. New York: John Wiley & Sons, Inc.

[4] Janiszewski Jacek. 2012. *Badania materiałów inżynierskich w warunkach obciążenia dynamicznego*. Warszawa: Wydawnictwo Wojskowej Akademii Technicznej.

[5] Kolsky Herbert. 1949. An investigation of the mechanical properties of materials at very high rates of loading. *Proc. Phys. Soc. Lond.* B 62 : 676.

[6] Weinong W. Chen, Bo Song. 2011. *Split Hopkinson (Kolsky) Bar: Design, Testing and Applications*. New York, Dordrecht, Heidelberg, London: Springer.

[7] Bhadeshia Harshad, David Edmonds. 1979. "The Bainite Transformation in a Silicon Steel". *Metallurgical Transactions A* 10A: 895.

[8] Bhadeshia Harshad. 1982. "Thermodynamic analysis of isothermal transformation diagrams". *Metal Science* 16(3) : 159.

[9] Bhadeshia Harshad, David Edmonds. 1983. “Bainite in silicon steels: new composition; property approach Part 1”. *Met. Sci*. 17(9) : 411.
[10] Bhadeshia Harshad, John Christian. 1990. “Bainite in steels”. *Metallurgical Transactions A* 21(3) : 767.
[11] Bhadeshia Harshad. 2005. “Bulk nanocrystalline steel”. *Ironmaking & Steelmaking* 32(5) : 405.
[12] Bhadeshia Harshad, Peter Brown, Carlos Garcia-Mateo. 2010. “Bainite steel and methods of manufacture therof”. Patent GB2462197.
[13] Garbarz Bogdan. *Technologia wytwarzania supertwardych materiałów nanostrukturalnych ze stopów żelaza oraz ich zastosowanie w pancerzach pasywnych i pasywno-reaktywnych*. Raport dotyczący projektu POIG.01.03.01-00-042/08, 2009-2013. Praca niepublikowana.
[14] Garbarz Bogdan, Wojciech Burian. 2014. “Microstructure and Properties of Nanoduplex Bainite–Austenite Steel for Ultra-High-Strength Plates”. *Steel Research Int.* 85(12) : 1620.
[15] Patent IMŻ na podstawie zgłoszenia nr P. 394037 (UP RP) z dnia 25.02.2011: *Stal bainityczno-austenityczna i sposób wytwarzania z tej stali blach*; Zgłoszenie patentowe IMŻ nr P. 396431 (UP RP) z dnia 26.09.2011: *Sposób obróbki cieplnej stali bainityczno-austenitycznej*; Zgłoszenie patentowe IMŻ nr P.407091 (UP RP) z dnia 6.02.2014: *Sposób obróbki cieplnej wyrobów z ultrawytrzymałej stali średniostopowe*j; Prawo ochronne UP RP na znak towarowy NANOS-BA®, udzielone od dnia 14.11.2011 (klasa towarowa: 06 blachy stalowe – blachy stalowe o dużej wytrzymałości i plastyczności).
[16] Marcisz Jarosław. *Opracowanie nowoczesnej konstrukcji modułu pancerza odpornego na udarowe oddziaływanie strumienia kumulacyjnego i pocisków*. Raport dotyczący projektu nr INNOTECH-K1/IN1/27/150443/NCBR/12, 2012-2015. Praca niepublikowana.
[17] Marcisz Jarosław. *Opracowanie technologii produkcji lekkiego kontenera obserwacyjno-obronnego (LOOK) ze stali nanostrukturalnych ultrawytrzymałych*. Raport dotyczący projektu nr POIR 04.01.04-00-0047/16, 2017-2020. Praca niepublikowana.
[18] Marcisz Jarosław, Bogdan Garbarz, Wojciech Burian, Adam Wiśniewski. 2011. New Generation Maraging Steel and High-Carbon Bainitic Steel for Armours. In *Proceedings of the 26th International Symposium on Ballistics*. Miami-Florida, USA: 1595.
[19] Marcisz Jarosław, Wojciech Burian, Jerzy Stępień, Lech Starczewski, Małgorzata Wnuk, Jacek Janiszewski. 2014. Static, dynamic and ballistic properties of bainite-austenite steel for armours. In *Proceedings of the 28th International Symposium on Ballistics*. Atlanta, USA: 1348.
[20] Burian Wojciech, Jarosław Marcisz, Bogdan Garbarz, Lech Starczewski 2014. “Nanostructured bainite-austenite steel for armours construction”. *Archives of Metallurgy and Materials* 59(3) : 1211.

[21] Marcisz Jarosław, Jacek Janiszewski, Wojciech Burian, Bogdan Garbarz, Jerzy Stępień, Lech Starczewski. 2015. „Badania właściwości dynamicznych wysokowytrzymałej stali nanostrukturalnej". *Prace Instytutu Metalurgii Żelaza* 67(2) : 96.

[22] Marcisz Jarosław, Wojciech Burian, Jacek Janiszewski, Radosław Rozmus R. 2017. „Microstructural changes of the nanostructured bainitic steel induced by quasi-static and dynamic deformation". *Archives of Metallurgy and Materials*. 62(4) : 2317.

Zmiany właściwości mechanicznych ultrawytrzymałej stali nanostrukturalnej w wyniku wielokrotnego odkształcenia dynamicznego

Jarosław MARCISZ[1], Bogdan GARBARZ[1], Jacek JANISZEWSKI[2]

[1]*Instytut Metalurgii Żelaza im. Stanisława Staszica*
ul. K. Miarki 12-14, 44-100 Gliwice
[2]*Wojskowa Akademia Techniczna, Wydział Mechatroniki i Lotnictwa*
ul. gen. Witolda Urbanowicza 2, 00-908 Warszawa 46

Streszczenie. W artykule przedstawiono wyniki badań nanostrukturalnej stali bainitycznej poddanej wielokrotnym odkształceniom dynamicznym z zastosowaniem metody pręta Hopkinsona oraz próby ściskania jednoosiowego próbki walcowej w symulatorze Gleeble. Stal o składzie chemicznym Fe-0,58%C-1,80%Si-1,95%Mn-1,3Cr-0,7Mo (% masowe) po wygrzewaniu izotermicznym w temperaturze 210°C charakteryzują następujące właściwości mechaniczne wyznaczone w statycznej próbie rozciągania: $R_{p0,2}$ = 1,3 GPa; R_m = 2,05 GPa; wydłużenie całkowite A = 12%, twardość 610 HV oraz udarność KV+20°C = 24 J i KV-40°C = 14 J. Analizie poddano krzywe naprężenie-odkształcenie uzyskane dla materiału wstępnie odkształconego przed kolejnym ściskaniem dynamicznym oraz po ściskaniu wielokrotnym. Próbki po odkształceniu poddano badaniom mikrostruktury w obszarach oddziaływania dynamicznego. Określono wpływ dynamicznych obciążeń wielokrotnych na zmiany charakterystyk badanego materiału, m.in. na mechanizm umocnienia odkształceniowego. Wyznaczono odkształcenie krytyczne dla stali nanostrukturalnej zależne od prędkości odkształcenia wynoszące 5,3% (910 s^{-1}) oraz ok. 10% (50 s^{-1}). Przekroczenie odkształcenia krytycznego w warunkach powtórnego jednoosiowego ściskania dynamicznego, skutkuje spadkiem zdolności stali do odkształcenia plastycznego i umocnienia odkształceniowego.

Słowa kluczowe: inżynieria materiałowa, stal nanostrukturalna, odkształcenie dynamiczne, adiabatyczne pasma ścinania